Hamiltonian approach to the dissociation of a coupled nonlinear exciton-vibron system

D. Hennig,[1,2,4] G. P. Tsironis,[1,2,3] and H. Gabriel[4]
[1]*Computational Physics Laboratory, Department of Physics, University of North Texas, Denton, Texas 76203*
[2]*Research Center of Crete, P.O. Box 1527, 71110 Heraklion-Crete, Greece*
[3]*Department of Physics, University of Crete, 71409 Heraklion-Crete, Greece*
[4]*Freie Universität Berlin, Fachbereich Physik, Institut für Theoretische Physik, Arnimallee 14, 14195 Berlin, Germany*
(Received 18 June 1993; revised manuscript received 1 December 1993)

We study the dissociation dynamics of polyatomic molecules using a Hamiltonian approach. Our model system consists of two molecular units, each having one electronic or vibrational state. An excitation is transferred between these two states with transfer matrix elements that depend on the intermolecular distance. The coupling with the intramolecular vibrations is included approximately through a cubic nonlinearity term while the intermolecular oscillations take place in a Morse potential. Dissociation in this model is a direct outcome of the coupling between the excitonic and vibrational subsystems leading to an energy exchange between the two. For small values of the transfer matrix elements we use the Melnikov function approach and show analytically the presence of homoclinic chaos in the system leading to dissociation for some bond configurations. The initial state preparation can drastically alter the dissociation process. We find that excitonic delocalization leads to enhanced dissociation rates. For larger intersite matrix elements we use the Chirikov overlap criterion to predict the onset of global phase space stochasticity, leading to dissociation for most bond lengths. The coupling to the intramolecular vibrations is seen to have an important effect on the dissociation phenomenon.

PACS number(s): 05.45.+b, 03.20.+i, 87.10.+e

I. INTRODUCTION

The standard theory of photodissociation of diatomic molecules has been developed by Freed, Band, and collaborators [1–4]. Recent advances in the theory of Hamiltonian systems, however, led researchers into new approaches for the classical dissociation problem dealing specifically with unimolecular reactions for weakly bound van der Waals systems. These approaches which use phase space transport concepts, such as homoclinic tangles and turnstiles, have been more successful than classical statistical dissociation theories in obtaining rates that are closer to experiment. The prototypical case of an HeI_2 molecule studied by Gray, Rice, and Noid [5] as well as Davis and Gray [6] has shown that phase space methods predict dissociation rates within a few percent of the ones obtained from numerical simulations, whereas the classical Rice, Ramsperger, Kassel, and Markus (RRKM) [7] method misses by at least two orders of magnitude. The initial success of the idea of the dissociation rate being proportional to the turnstile area around the separatrix that forms a bottleneck for the molecular dissociation led to a large number of similar studies that use phase space methods. These studies address either specific chemical systems or analyze the dissociation dynamics from a more abstract perspective for model systems that contain some general features. The models in the latter category assume, as a rule, that the potential between the two molecular species is of the Morse type. These models fall into two different classes: (i) the single one-degree-of-freedom Morse oscillator itself, whose clear-cut separation into bounded and unbounded motion is destroyed by external periodic [8–14] or quasiperiodic forcing [15–17] as well as by exposing the system to periodically kicked impulses [18–21] and (ii) Hamiltonian model systems with at least two degrees of freedom based on several assumptions as to the form of the coupling [5,6,21–26].

Most of these pioneering studies have not addressed specifically the possibility of dissociation from the coupling of the intermolecular vibrational modes to excitonic (electronic or vibrational) transfer between the two molecular units. This coupling, which arises as a result of the dependence of the excitation on relative vibrational deformations, leads to a modulated exciton transfer between the two molecular units. Typical examples of such a situation present organic molecules that form dimers such as formamide, dichloromethane, and others. In the case of the formamide dimer in particular, a vibrational excitation (Amide I) is transferred between the two monomers that are in a Morse potential [27]. In addition to the exciton transfer problem, the interaction of the excitons with local intramolecular oscillations can be also included. The incorporation of the exciton transfer problem in the dissociation studies enhances the complexity of the problem and introduces new questions. In particular, the role of the energy exchange between the excitonic and vibrational degrees of freedom in the dissociation process needs to be understood. The issues associated with the latter question are the primary target of the present paper.

Our molecular model consists of two units (atoms, molecules, or clusters of molecules) that interact via a van der Waals-type interaction. We will follow the literature in assuming that the two units are vibrationally coupled through a Morse potential (see, e.g., [5,6]). We assume further that each unit has only one electronic state acces-

sible for an electron (or, in general, an excitation) to transfer between the units. The matrix elements for the transfer between the two units depends on the distance between them. Since the latter is not constant, the transfer matrix elements are also modulated by the motion of the two sites relative to each other. When the two units are further apart, the matrix elements diminish, leading to a reduction in excitonic transfer from one site to the other. When, on the other hand, the two sites are closer to each other, we have an increase in the excitonic transfer. Finally, we also take into account the interaction of the excitation with the local vibrational modes of each molecular unit. In the limit where the local oscillators adjust to the excitonic deformation much faster than the latter moves to the neighboring site, we can incorporate the effect of the oscillators by adding a cubic nonlinearity term in the equation for the excitonic problem [28–31]. Our model for a dissociating molecule consists, therefore, of two well-established limits. When the effects of the electronic (or vibrational) excitation are ignored, we recover the well-known case of two molecular units that are vibrationally coupled through a Morse potential. When, on the other hand, the intermolecular vibrations are omitted, we obtain the equations for electronic transfer additionally modified by the local intramolecular vibrations. In the limit studied here, where the time scale of the latter is taken to be much faster than that of the exciton, we recover the nonlinear dimer system described by the discrete nonlinear Schrödinger equation (DNLS) [30,32,33]. By including the excitonic transfer (additionally modified by the nonlinear term to include polaronic-type effects) in the vibrational dissociation problem, we can accomplish a more realistic description of induced dissociation. We can address the important question of the influence of the excitation transfer in the bond breaking process and in particular we can study the energy exchange between excitonic and vibrational degrees of freedom. For appropriately initially prepared excitonic states there can be a maximization of energy redistribution leading to faster dissociation.

In our model, dissociation results from the coupling of the excitonic with the vibrational degrees of freedom. The dissociation bottleneck is provided essentially by the Morse potential, whereas homoclinic chaos and the presence of the turnstiles is an outcome of the nonlinearity in the exciton transfer problem. In addition to the amount of nonlinearity, the initial excitonic preparation plays an important role in the dissociation rate. Analytical as well as numerical predictions for dissociation rates are obtained for different parameter values. The structure of the paper is the following: In Sec. II we introduce the model, discuss the various parameters and approximations involved, and derive the dynamical equations for the vibrational and excitonic problems. Subsequently, in Sec. III we introduce the Melnikov method and obtain predictions for the onset of the dissociation induced by homoclinic chaos, and discuss the role of the initial preparation of the system in the dissociation process. In Sec. IV we discuss the case of fully developed bond chaos and obtain predictions using the Chirikov overlap criterion. In Sec. V we give our conclusions.

II. MODEL FOR THE WEAKLY BOUND MOLECULAR DIMER

We consider the exchange of excitonic and vibrational energy between two polyatomic molecules interacting via weak van der Waals forces and forming a weakly bound molecular dimer. The model Hamiltonian is

$$H = H_{\text{exc}} + H_{\text{vib}} , \tag{1}$$

with H_{exc} being the two site nonlinear exciton Hamiltonian related to a DNLS equation [30]:

$$H_{\text{exc}} = E^0_{\text{exc}}[|c_1|^2+|c_2|^2] - \tfrac{1}{2}\chi[|c_1|^4+|c_2|^4] - V[c_1^* c_2 + c_1 c_2^*] . \tag{2}$$

The first term in Eq. (2) represents the diagonal part of the Hamiltonian for the local electronic (vibrational) excitation in the molecular dimer, with c_n being the probability amplitude of the excitation to be at site n and E^0_{exc} the corresponding on-site energy. The off-diagonal part of Eq. (2) describes the transfer of the exciton between the two sites, with V being the corresponding transfer matrix element that arises as a result of a dipole-dipole interaction. The additional terms in the excitonic Hamiltonian originate from an adiabatic elimination of the fast intramolecular vibrations and represent the energy lowering of the local excitation energy due to strong coupling to the corresponding local vibrational modes. These terms are responsible for the nonlinearity in the equations of motion. The derivation of this nonlinear exciton model is based on a time-scale separation argument and in particular on the fact that the intramolecular vibrations are much faster than any intermolecular processes (intermolecular excitonic transfer or the relative vibrational motion of the monomers) [28,29,31]. This reasonable assumption is justified by the relatively small reduced masses involved in the intramolecular vibrations as well as the large magnitude of the exciton-vibration coupling constants on one side, whereas, on the other side, the intermolecular vibrational modes are of low frequency due to the larger masses of the two monomers and the weakness of the bond between them. The nonlinearity parameter represents a sum over the square of the intramolecular coupling strengths divided by the corresponding vibrational frequencies. Thus, the influence of the intramolecular vibrational modes is incorporated in this model as a static nonlinear modulation of the excitonic on-site energy with strength χ. For an appropriate description of the exciton dynamics, we introduce the following real valued Bloch variables:

$$x = c_1^* c_2 + c_1 c_2^* ,$$
$$y = i[c_2^* c_1 - c_2 c_1^*] ,$$
$$z = |c_1|^2 - |c_2|^2 ,$$

satisfying the identity $x^2+y^2+z^2=1$. The dynamics of the excitonic probability amplitudes is then described by rotation of a vector lying on the surface of a three dimensional sphere and is analogous to the dynamics of a classical spin. The time evolution of the Bloch vector

$\mathbf{r}=(x,y,z)$ is governed by

$$\frac{d\mathbf{r}}{dt}=-\mathbf{r}\times\partial H/\partial\mathbf{r}\ , \tag{3}$$

with the Hamiltonian

$$H_{\rm exc}=-\tfrac{1}{2}\chi(1+z^2)-2Vx\ . \tag{4}$$

In the weakly bound dimer system the vibration of the monomers is described through the relative coordinate q with a Hamiltonian given by

$$H_{\rm vib}=\frac{1}{2\mu}p^2+D\{1-\exp[-a(q-q_0)]\}^2\ . \tag{5}$$

In Eq. (5), q_0 is the equilibrium position of the Morse potential, p is the canonical momentum conjugate to q, μ is a reduced mass, D is the dissociation energy, and a is the range parameter of the Morse potential. The excitonic transfer matrix element depends on the intersite distance in an exponential manner:

$$V(q)=V_0\exp[-a(q-q_0)]\ . \tag{6}$$

It is through Eq. (6) that the coupling between excitonic and intersite vibrational degrees of freedom is introduced. In order to minimize the number of parameters in our model, we set the range parameter of the transfer integral equal to the range parameter of the Morse potential. The bond-vibration dynamics is influenced strongly by the distance, and the exciton mobility can be substantially reduced with increasing distance. In return, the excitonic motion modulates the Morse potential of the intersite vibration. We neglect here the dependence of the excitonic on-site energies on the intersite distance since this is a minor effect compared to the nonlinear energy lowering due to strong coupling to the intramolecular modes. For small deviations from the equilibrium bond distance q_0, we get approximately linear distance dependence for the transfer matrix discussed in an earlier paper in the context of exciton transfer in [34].

To simplify the notations, we express the Hamiltonian in units of $2D$, i.e., $\overline{H}\rightarrow H/2D$, introduce further the following dimensionless variables $a(q-q_0)\rightarrow\bar{q}$ and $p/\sqrt{2D\mu}\rightarrow\bar{p}$, and finally we drop the overbars. We scale time as $t\rightarrow\omega_0 t$, where $\omega_0=\sqrt{2a^2D/\mu}$ is the frequency of the Morse oscillator in the harmonic approximation, and obtain the following set of equations of motion describing fully the dynamics of the coupled exciton-vibron model:

$$\dot{x}=\gamma yz\ , \tag{7}$$

$$\dot{y}=-\gamma xz+2V\exp(-q)z\ , \tag{8}$$

$$\dot{z}=-2V\exp(-q)y\ , \tag{9}$$

$$\dot{q}=p\ , \tag{10}$$

$$\dot{p}=-[\exp(-q)-\exp(-2q)]-2V\exp(-q)x\ . \tag{11}$$

We defined $V=V_0/2D$ and $\gamma=\chi/2D$. The intersite distance enters via the q dependence of the transfer matrix element in the equations for the excitonic Bloch variables, while the excitonic off-diagonal variable x acts like a source term in the bond oscillator equation. The Hamiltonian for the dynamical system in Eqs. (7)–(11) is

$$H=\tfrac{1}{2}p^2+\tfrac{1}{2}[1-\exp(-q)]^2+E^0_{\rm exc}-\tfrac{1}{2}\gamma(1+z^2)-2V\exp(-q)x\ . \tag{12}$$

This Hamiltonian system possesses two first integrals of motion, viz., the energy ($H=$const) and the norm of the Bloch vector $x^2+y^2+z^2=1$. Therefore, it represents a two-degrees-of-freedom Hamiltonian system that is integrable in two cases: (i) when the nonlinearity parameter is zero, i.e., $\gamma=0$, and/or (ii) for vanishing transfer matrix element $V=0$. In the first case we get with $x=$const an additional first integral and the system can be immediately integrated, whereas in the second case the Morse oscillator decouples from the excitonic degree of freedom and the occupation difference z becomes a further integral. In the following sections we investigate the dynamics of the coupled exciton-vibration system starting from the integrable case (ii) of vanishing transfer matrix element and treating V as a perturbation parameter. For an application of the perturbation methods it is convenient to pass canonically to action-angle variables for the excitonic subsystem. From the equations of motion we see that for zero transfer integral V the motion of the Bloch vector is restricted to a rotation on the circle

$$[x(t)]^2+[y(t)]^2=1-[z(0)]^2$$

in the planes of constant (angular momentum z, i.e., $z(0)=z(t=0)$. The Bloch vector then rotates around the z axis with frequency $-\gamma z(0)$. We can therefore take z as the action variable J_1, i.e., $z=J_1$, and introduce the corresponding canonical angle variable via the relations $x=\sqrt{1-J_1^2}\cos\theta_1$ and $y=\sqrt{1-J_1^2}\sin\theta_1$. The Hamiltonian (12) expressed in action-angle variables for the excitonic subsystem is given by

$$H^\epsilon=H_M(p,q)+H_{\rm exc}(J_1)+\epsilon H^1(q,J_1,\theta_1)\ , \tag{13}$$

consisting of the part for the unperturbed Morse oscillator

$$H_M(p,q)=\tfrac{1}{2}p^2+\tfrac{1}{2}[1-\exp(-q)]^2\ , \tag{14}$$

the excitonic part

$$H_{\rm exc}(J_1)=E^0_{\rm exc}-\tfrac{1}{2}\gamma(1+J_1^2)\ , \tag{15}$$

and the interaction part

$$H^1(q,J_1,\theta_1)=-2V\exp(-q)\sqrt{1-J_1^2}\cos\theta_1\ . \tag{16}$$

We introduced in Eq. (13) the small dimensionless parameter $\epsilon\ll 1$ to emphasize the perturbative character of the exciton-vibration coupling term. Due to the symmetry $J_1\rightarrow -J_1$, we consider in what follows only excitonic occupations with $J_1>0$ yielding definite frequencies $\omega_1=-\gamma J_1<0$.

Before proceeding with an analysis of the coupled dynamics, we discuss briefly the geometrical structure of the unperturbed phase space which is four dimensional and is given by

$$(p,q,J_1,\theta_1)\in\mathbb{R}^2\times\mathbb{R}^1\times S^1\ . \tag{17}$$

The phase space of the unperturbed Morse oscillator has a center at $(p,q)=(0,0)$ and an unstable nonhyperbolic fixed point at ($p=0$, $\lim q\to\infty$). The coordinates of the homoclinic orbit corresponding to the fixed point at infinity are given by

$$q^h(t)=\ln\left[\frac{1+(t-t_0)^2}{2}\right], \tag{18}$$

$$p^h(t)=\frac{2(t-t_0)}{1+(t-t_0)^2}, \tag{19}$$

where t_0 is the time along the unperturbed flow parametrizing the homoclinic orbit. The full unperturbed system has an invariant two-dimensional nonhyperbolic manifold:

$$\mathcal{M}=\{(p,q,J_1,\theta_1)\in\mathbb{R}^2\times\mathbb{R}^1\times S^1 | p=0,\lim q\to\infty\}, \tag{20}$$

and the unperturbed orbits in the homoclinic manifold are given by

$$(p,q,J_1,\theta_1)=(p^h(t-t_0),q^h(t-t_0),J_1,\omega_1 t+\theta_1^0). \tag{21}$$

By fixing the phase θ_1^0, we restrict the study of the dynamics to a three-dimensional surface of section $\Sigma^{\theta_1^0}$, where

$$\Sigma^{\theta_1^0}=\{(p,q,J_1,\theta_1)|\theta_1=\theta_1^0\in[0,2\pi)\}. \tag{22}$$

The associated Poincaré map is defined by

$$P:\Sigma^{\theta_1^0}\to\Sigma^{\theta_1^0}. \tag{23}$$

Since the trajectories are confined to motions in the three-dimensional total-energy manifold

$$H(p,q,J_1)=h=\text{const},$$

which is transverse to $\Sigma^{\theta_1^0}$, an additional dimension is reduced and the Poincaré map $\Sigma_h^{\theta_1^0}=\Sigma^{\theta_1^0}\cap h$ is actually two dimensional, parametrized by the Morse oscillator variables (p,q). In the following sections we denote the cross section by $\Sigma^{\theta_1^0}$.

For $\epsilon=0$ the unperturbed Poincaré map possesses an unstable nonhyperbolic fixed point with coinciding stable and unstable manifolds forming a two-dimensional homoclinic separatrix. In Sec. III we turn to the dynamics of the coupled oscillators where we focus on the phenomenon of dissociation caused by chaotic transport associated with the homoclinic tangle around the perturbed separatrix.

III. MELNIKOV METHOD AND HOMOCLINIC CHAOS INDUCED MOLECULAR DISSOCIATION

A. Chaotic transport

In this section we use the Melnikov method to prove the existence of homoclinic chaos in the coupled exciton bond-vibration dynamics. We saw in Sec. II that in the limit of vanishing transfer matrix element, the coupled exciton-bond oscillator dynamics decouples completely. The resulting two independent integrable systems, viz., the system of the isolated monomers and the Morse oscillator system, conserve the on-site energy $H_{\text{exc}}(J_1)$ and the bond energy $H_M(p,q)$, respectively. The phase space of the isolated Morse oscillator is divided into regions of bounded and unbounded motion by a separatrix corresponding to a homoclinic orbit with the dissociation energy $H_M=\frac{1}{2}$. Bounded motion inside the separatrix is characterized by a bond energy $H_M<\frac{1}{2}$, representing a stable molecular dimer configuration, whereas an unbounded orbit with $H_M>\frac{1}{2}$ corresponds to a dissociated molecular dimer. Since the energy of the isolated Morse oscillator is conserved, a bounded orbit is constrained to motion inside the separatrix and molecular dissociation is excluded. Thus the separatrix acts as a complete barrier in phase space separating the bounded and unbounded motion. This stable situation drastically changes when the coupling between the Morse oscillator and the excitonic degree of freedom is turned on. Provided enough excitonic energy is initially injected in the monomers, parts of this energy can flow into the weak bond leading to a bond breakup and molecular dissociation. This phenomenon is directly related to the destruction of the separatrix of the Morse oscillator.

For $\epsilon\neq0$ the stable and unstable manifolds of the homoclinic structure on the Poincaré map may intersect transversally, leading to the onset of homoclinic chaos. The analysis is based on the properties of the generalized Melnikov function [35]. For our two-degrees-of-freedom system the generalized Melnikov integral is given by

$$M(\theta_1^0,t_0)=-\int_{-\infty}^{\infty}dt\, D_{\theta_1}H^1(p^h(t),q^h(t);J_1,\omega_1 t+\theta_1^0+\omega_1 t_0), \tag{24}$$

where this integral is evaluated on the unperturbed homoclinic manifold. Using Eqs. (14)–(16) and (18) and (19), we obtain

$$M(\theta_1^0,t_0)=-4V\pi\gamma J_1\sqrt{1-J_1^2}\exp(-\gamma J_1)\times\sin[\theta_1^0+\omega_1 t_0]. \tag{25}$$

The Melnikov function has simple zeros and thus homoclinic chaos is present in our model. We now come to the consequences of the manifold separation in the bond dynamics. Due to the resulting nonintegrable motions, the stable and unstable manifolds of the homoclinic separatrix on $\Sigma^{\theta_1^0}$ are no longer identical and intersect each other, establishing a homoclinic tangle in the vicinity of the broken separatrix. The Melnikov amplitude increases with increasing V and gives via

$$d(t_0)=M(t_0)/\|DH(p^h(-t_0),q^h(-t_0))\|$$

an $O(\epsilon)$ estimate of the separation of the perturbed stable and unstable manifolds at the point $(p^h(-t_0),q^h(-t_0))$ on the unperturbed separatrix [36,37,35]. D is the (p,q) gradient and $\|\ \|$ is the Euclidean norm in $\mathbb{R}^2$. The manifold separation is influenced by the excitonic action J_1 and frequency $|\omega_1|=\gamma J_1$. This is shown in Fig. 1, where the absolute value of the amplitude of the Melnikov func-

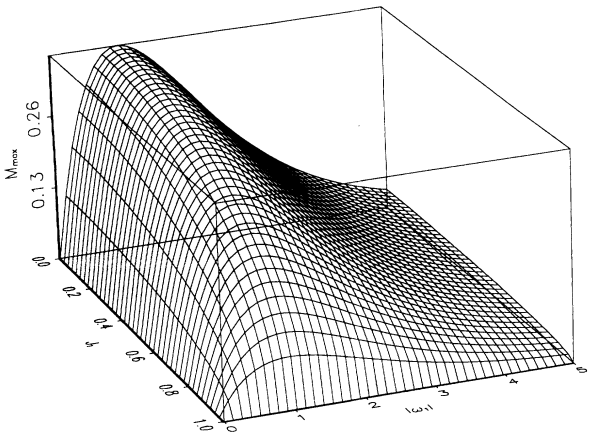

FIG. 1. The maximum amplitude of the Melnikov function in units of $4\pi V$ as a function of the action J_1 and the frequency $|\omega_1|=\gamma J_1$.

tion divided by $4\pi V$, i.e.,

$$\frac{|M_0(\gamma,J_1)|}{4\pi V}=\gamma J_1\sqrt{1-J_1^2}\exp(-\gamma J_1)\equiv M_{\max}\ , \qquad (26)$$

is plotted versus $|\omega_1|=\gamma J_1$ and J_1. (An analogous quantity is referred to as the *relative scaling function* in [17].)

The frequency dependence of the Melnikov amplitude regulates to what extent manifold separation and transport quantities are affected by the forcing excitonic motion, as will be discussed below. For large frequencies ω_1, the exponential decrease of the Melnikov amplitudes dominates, resulting in small separatrix splittings. Further increase of the frequency $|\omega_1|$ leads to vanishing splitting and the system approaches the integrable regime. In the opposite limit $\omega_1\to 0$, the Melnikov amplitude M tends also to zero. The most pronounced separatrix destruction appears at $|\omega_1|=\gamma J_1=1$.

Figure 2 shows part of the perturbed separatrix dynamics for a Poincaré map with a cross section determined by $\theta_1^0=\pi$. The separatrix is constructed by taking the union of segments of the stable and unstable manifold of the fixed point at infinity ($q\to\infty$, $p=0$). The manifolds were calculated by propagating a small line element starting at $q\geq 20$: for positive times along the unstable branch of the invariant manifold of the unperturbed separatrix with negative momentum, and backward in time for the stable branch with positive momentum until the two branches meet each other at a homoclinic point located at $p\simeq 0$, $q\simeq -0.693$. In this way we obtain the "exact" separatrix of the coupled dynamics. Further propagation of the stable (unstable) branch in the region of negative (positive) momentum yields the structure shown in Fig. 2, which is created by homoclinic oscillations resulting in transversal intersection of the stable and unstable manifolds at so-called *primary intersection points*. Parts of the stable and unstable manifold between two adjacent primary intersection points form the boundary of a *homoclinic lobe*. Adjacent lobes like those labeled by L_{ub} (unbounded to bounded) and L_{bu} (bounded to unbounded) in Fig. 2(a) have been called a *turnstile* by MacKay, Meiss, and Percival [39]. Iteration of each transverse intersection point yields new intersection of the stable and unstable branch and in the same manner the lobes evolve under the Poincaré map, thereby creating new lobes, as indicated in Fig. 2(a). The dynamics of the lobes and its relation to transport in phase space are, by now, well understood. We refer to Refs. [38–41] for details and, with reference to the turnstile of Fig. 2(a), merely mention that the lobe L_{bu} inside the separatrix is the outgoing flow which leaves the inner separatrix re-

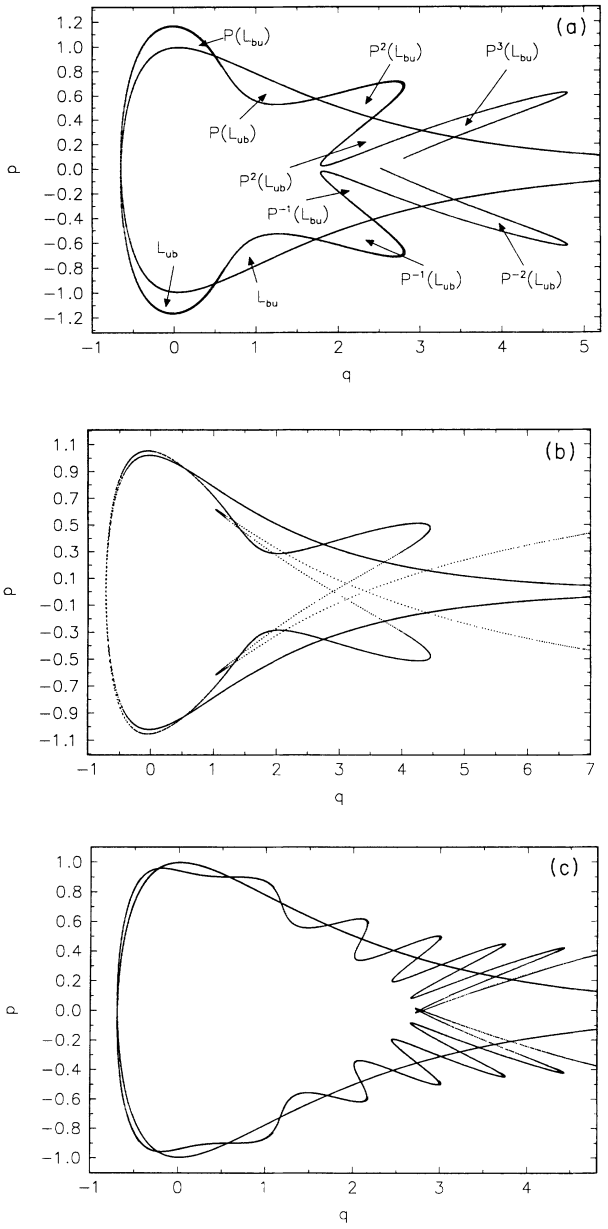

FIG. 2. Poincaré map corresponding to a cross section with $\theta_1^0=\pi$ showing the homoclinic tangle and the lobe structure for the perturbed separatrix of the Morse oscillator for $V=0.025$. We illustrated the dynamics of the turnstile lobes which are labeled by L_{bu} for the escape lobe and L_{ub} for the capture lobe, respectively. In (a), $J_1=0.80$, $\gamma=3$; in (b), $J_1=0.29$, $\gamma=3$; and in (c), $J_1=0.29$, $\gamma=1$. We note that the lobe area reduces for larger excitation localization or smaller nonlinearities.

gion per iteration. The lobe L_{ub} outside the separatrix is the flow mapped from the outer to the interior region of the separatrix. Since the Poincaré map is area preserving, each half of the turnstile has equal area, resulting in zero net flow across the separatrix.

B. Estimate of the dissociation rate

Since the turnstiles are gateways for the transport across the separatrix from bounded to unbounded motion and vice versa, i.e., for dissociation and recombination, the dissociation rates are determined by the corresponding turnstile flux escaping through the separatrix. The flux across the broken separatrix can be calculated analytically by using the Melnikov method [38,42] or by exact numerical computation of the turnstile areas.

We present an analytical approach for estimating the rate of dissociation of highly excited states of the Morse oscillator in the near integrable regime. Expressed in terms of the dynamics of the associated two-dimensional Poincaré map, computing the dissociation rate becomes equivalent to the transport problem: What fraction of points, initially bound in the interior of the separatrix, have escaped via the turnstile to the region of unbounded motion after a certain time interval? For a uniform distribution of points in phase space, the area of the escape turnstile lobes gives the amount of phase space transported across the separatrix after one iteration of the Poincaré map. In studies of molecular dissociation the Markov-model approach developed by MacKay, Meiss, and Percival [39] has often been employed to compute phase space transport rates in an associated two-dimensional area-preserving Poincaré map (see, e.g., [6,25]). Their Markov model is based on the picture that the Poincaré plane is divided into stochastic regions separated by partial barriers which are created by the intersecting stable and unstable manifolds of hyperbolic periodic orbits and cantori. Transport across these partial barriers takes place by mapping the corresponding turnstile lobes from one region to another where it is assumed that their contents are instantaneously and uniformly distributed by the mixing motion throughout the region they have entered. In their statistical theory for unimolecular decay of weakly bound van der Waals complexes, Davis and Gray invoked the concept of transport across bottlenecks in the relevant molecular phase space [6]. Based on a Hamiltonian description of the two-dimensional model for the van der Waals complex HeI_2, they obtained for unimolecular decomposition reasonable agreement between theoretical reaction rates and numerically determined on short time scales. In their work they used a statistical theory based on transport across a single dynamically determined separatrix (intermolecular bottleneck). For a more accurate modeling of decay that also holds for longer time scales, they solved kinetic schemes with the addition of intramolecular bottlenecks that are associated with the partial separatrices of resonances. Excellent agreement between the theory and numerical experiments was then obtained. This statistical theory has further successfully been applied in two-dimensional models to study the dynamics of unimolecular decay of other weakly bound van der Waals complexes, in intramolecular vibrational relaxation in OCS [43], isomerization [46,47], and biomolecular reactions [44,45].

Following Davis and Gray [6], we consider the fragmentation process of an ensemble of trajectories for the oscillator system of Eqs. (7)–(11). Assuming fast randomization of phase points in the stochastic region in a single iteration of the Poincaré map, the probability κ for escaping the separatrix per iteration is determined by

$$\kappa = A_{\text{lobe}} / A_{\text{st}} , \tag{27}$$

where A_{lobe} is the area of the escape lobe and A_{st} is the area of the chaotic region inside the separatrix. This transition region is enclosed by the dynamically determined separatrix excluding the region of bounded particle motions enclosed by the outermost Kol'mogorov-Arnol'd-Moser (KAM) torus [6,25]. For ϵ small, the area of the stochastic region A_{st} is determined by the area of homoclinic tangle A_{tangle} in the interior of the separatrix and can be computed via the Melnikov function since the maximum Melnikov amplitude determines how the stochastic layer ranges down into the inner region of the separatrix on a p-q Poincaré plane $\Sigma^{\theta_1^0}$. The lobe area on a Poincaré plane $\Sigma^{\theta_1^0}$ can be calculated with the help of the Melnikov function [48,49]:

$$A_{\text{lobe}} = \epsilon \int_{t_{0,1}}^{t_{0,2}} M(t_0) dt_0 + O(\epsilon^2) , \tag{28}$$

where $t_{0,j}$, $j=1,2$, are the zeros of the Melnikov function corresponding to two successive homoclinic intersection points of the manifolds. Using Eqs. (25) and (28), the lobe area is given by

$$A_{\text{lobe}} = \frac{2M_{\max}}{|\omega_1|} . \tag{29}$$

We note that we found very good agreement between the analytically determined lobe area given in Eq. (29) and the lobe area determined numerically from the Poincaré surface of section using a trapezoidal rule.

The area of the homoclinic tangle inside the separatrix is given by the difference of the area enclosed by the separatrix (s) and the area enclosed by the region of regular motion (r) inside the separatrix:

$$A_{\text{layer}} = \left[\oint_s - \oint_r \right] p \, dq . \tag{30}$$

The stochastic layer of the Poincaré plane inside the separatrix ranges from the separatrix level down to an energy given by the maximum Melnikov amplitude. This provides, for small numbers of iteration of the Poincaré map, a measure for the penetration of the level sets of the unperturbed Morse oscillator by the homoclinic tangle [17]. Thus, the approximate boundary of the regular region of the Poincaré plane is formed by an invariant curve corresponding to an orbit of the unperturbed Morse oscillator with energy

$$h = \tfrac{1}{2}\{p^2 + [1 - \exp(-q)]^2\} = \tfrac{1}{2}(1 - 2M_{\max})$$

and turning points

$$q_{\pm}=-\ln(1\pm\sqrt{1-2M_{\max}}),\quad p_{\pm}=0\ .$$

Taking this into account, we obtain

$$\begin{aligned}A_{\text{layer}}&=2\int_{-\ln[2(1-\tilde{V})]}^{\infty}\sqrt{[2(1-\tilde{V})\exp(-q)-\exp(-2q)]}dq\\&\quad-2\int_{q_+}^{q_-}\sqrt{[2\exp(-q)-\exp(-2q)]-2M_{\max}}dq\\&=2\pi[\sqrt{2M_{\max}}-\tilde{V}]\ ,\end{aligned}\tag{31}$$

with

$$\tilde{V}=2V\sqrt{1-J_1^2}\cos\theta_1^0\ .\tag{32}$$

The escape probability across the separatrix is given by

$$\kappa=\frac{M_{\max}}{\pi|\omega_1|[\sqrt{2M_{\max}}-\tilde{V}]}\ .\tag{33}$$

The decay rate is determined by the ratio of κ to the average time between two iterations of the Poincaré map. Rather than calculating an average return time for the Poincaré map, we estimate the rate by assuming that in the near integrable regime a trajectory passes the cross section at intervals given by the period of the unperturbed excitonic oscillator $T=2\pi/|\omega_1|$. This reasonable assumption is justified by the fact that in the transition region of chaotic motion, the excitonic action, i.e., J_1, remains almost constant for small transfer matrix elements. (See also Ref. [6] for a similar argument in the context of vibrational van der Waals predissociation.) For the decay rate we obtain

$$K=\frac{\kappa}{T}=\frac{1}{2\pi^2}\frac{M_{\max}}{[\sqrt{2M_{\max}}-\tilde{V}]}\ .\tag{34}$$

To compare the analytically estimated rates with numerical escape probabilities, we compute the lifetime of an ensemble of trajectories corresponding to a level set of the unperturbed Hamiltonian $E_0=E_M+E_{\text{exc}}$. According to Ref. [6], this is done by the following.

(i) Generating a set of initial conditions corresponding to solutions contained in the stochastic region inside the dynamically determined "exact" separatrix on a Poincaré plane $\Sigma^{\theta_1^0}$:

$$E_M=\tfrac{1}{2}\{p_j^2+[1-\exp(-q_j)^2]\},\quad j=1,N\tag{35}$$

where N is the number of initial points on a level set E_M of the unperturbed Morse oscillator. On the level set E_M the points (p_j,q_j) are sampled by varying the respective angle variable in even steps between 0 and 2π, keeping the action fixed, thus leading to a weighted distribution of initial points on the Poincaré plane.

(ii) Integrating numerically the system given in Eqs. (7)–(11), following each trajectory, and observing the time it takes to escape the region of bounded motion. Fragmentation is assumed to be accomplished for $q>15$ and $p>0$. The survival probability is the lifetime averaged over an ensemble of initial conditions, i.e.,

$$P(t)=\ln[N(t)/N(0)]\ ,$$

where $N(t)$ is the number of trajectories which have not led to fragmentation and $N(0)$ is the number of initial conditions. In Fig. 3 the survival probability is displayed for different initial excitonic preparations J_1. These curves show exponential decay on short time scales. The corresponding fragmentation rates can be obtained from the slope of a linear fit of the decay curves shown in Fig. 3 together with the rate determined analytically from Eq. (34), but shifted to the onset of fragmentation in the numerical calculations. The analytical estimated fragmentation rates are in fairly good agreement with those obtained from numerical simulations. For a critical discussion of the Markov model and exact computation of transport rates based on the topology of lobe intersections, see Wiggins [38], Beige, Leonard, and Wiggins [50], and Rom-Kedar, Leonard, and Wiggins [48].

IV. TRANSITION TO GLOBAL CHAOS

In Sec. III we proved analytically through the Melnikov method the existence of homoclinic chaos in the coupled exciton bond-oscillator dynamics in the near integrable regime. We further demonstrated this numerically by showing the destruction of the unperturbed separatrix of

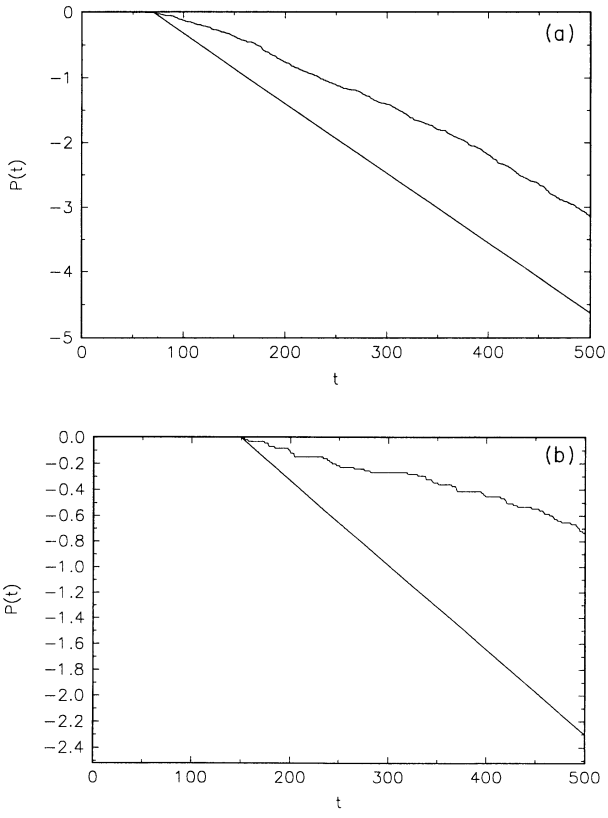

FIG. 3. The survival probability $P(t)$ for an ensemble of 3000 trajectories. The analytically predicted dissociation rates obtained from Eq. (34) are shown as straight lines lying below the numerically determined decay curves. The parameters are $E_M=0.49$, $\gamma=3$, and $V=0.025$. In (a), $J_1(0)=0.3$ and in (b), $J_1(0)=0.8$.

the Morse oscillator in a short interval of time (for small number of Poincaré map iterations). The resulting irregular dynamics provides a mechanism for escape from bounded to unbounded solutions for bond configurations with energy that is close to the dissociation threshold. Dissociation is, however, also possible for smaller bond lengths that are close to the equilibrium bond configuration. For this to happen, the chaotic dynamics must cover extended regions of phase space. The extension of chaos grows as the magnitude of the perturbation increases, leading to regions of local stochasticity divided by KAM surfaces. The outermost KAM torus, in particular, poses a complete barrier to the lobe penetration of the level sets of the unperturbed Morse oscillator [17]. As the perturbation strength increases, the KAM tori located in between neighboring resonances get destroyed due to resonance overlap, leading to widespread chaos. The critical perturbation for the occurrence of the resonance overlap can be estimated through the use of the Chirikov criterion [14,51].

For an analysis of the coupled dynamics in this regime, we now introduce the action-angle variables for the vibrational degree of freedom:

$$q(J_2,\theta_2)=\ln\frac{1-\sqrt{2E_M}\cos\theta_2}{1-2E_M} , \tag{36}$$

$$p(J_2,\theta_2)=\frac{\sqrt{1-2E_M}\sqrt{2E_M}\sin\theta_2}{1-\sqrt{2E_M}\cos\theta_2} . \tag{37}$$

In Eqs. (36) and (37), E_M is the unperturbed energy of the Morse oscillator that depends only on the action J_2:

$$E_M=J_2(1-\tfrac{1}{2}J_2) . \tag{38}$$

With this definition, we now have the following Hamiltonian for the coupled dynamics:

$$\begin{aligned}H&=E^0_{\rm exc}-\tfrac{1}{2}\gamma-\tfrac{1}{2}\gamma J_1^2+J_2(1-\tfrac{1}{2}J_2)\\&\quad-\epsilon 2V\sqrt{1-J_1^2}\sum_m W_m(J_2)\cos[\theta_1+m\theta_2]\\&=H^0(J_1,J_2)+\epsilon H^1(J_1,J_2,\theta_1,\theta_2) ,\end{aligned} \tag{39}$$

where the coupling term has been expanded into a Fourier series with expansion coefficients given by

$$W_m(J_2)=\frac{1}{2\pi}\int_0^{2\pi}d\theta_2 e^{im\theta_2}\exp[-q(J_2,\theta_2)] \tag{40}$$

$$=\sqrt{1-2E_M}\left[\frac{1-\sqrt{1-2E_M}}{1+\sqrt{1-2E_M}}\right]^{m/2} . \tag{41}$$

In the uncoupled integrable case the actions of the excitonic and vibrational systems are conserved and the angles oscillate with frequencies determined by

$$\omega_i(J_i)=\partial H^0(J_1,J_2)/\partial J_i ,$$

yielding 2π-periodic solutions $\theta_i=\omega_i(J_i)t+\theta_i^0$. The unperturbed frequencies of θ_1 and θ_2 are

$$\omega_1(J_1)=-\gamma J_1 \tag{42}$$

and

$$\omega_2(J_2)=(1-J_2) , \tag{43}$$

respectively. The excitonic transfer matrix element V couples nonlinearly the oscillations of the angles θ_1 and θ_2 and causes variations of the actions J_1 and J_2 proportional to V. The effect of the coupling is maximized when the phases in the Fourier series expansion do not vary rapidly and the two systems are coupled resonantly. The condition for the occurrence of such a primary resonance is determined by the stationary phase condition in the Fourier series expansion of the perturbation:

$$\frac{d}{dt}(\theta_1+m\theta_2)=0 , \tag{44}$$

$$m\omega_2(J_2)+\omega_1(J_1)=0 . \tag{45}$$

The resonance surfaces in the two-dimensional action space are given by

$$\gamma J_1=m(1-J_2) \tag{46}$$

and are plotted in Fig. 4 together with some level curves of the unperturbed Hamiltonian $H^0(J_1,J_2)$ for $\gamma=1$. We note that for higher excitonic action J_1, the positions of

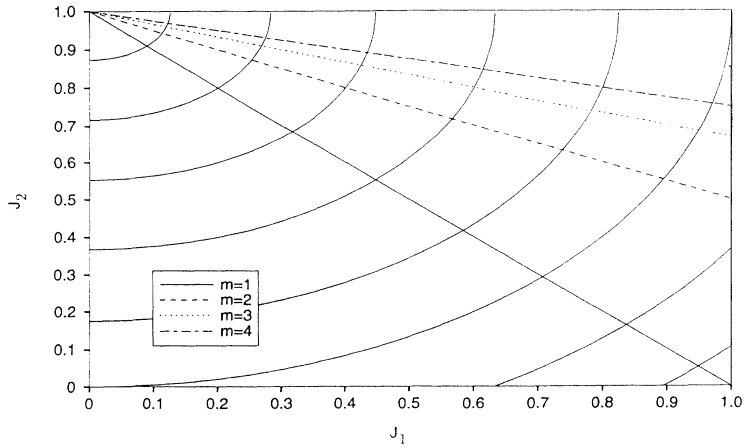

FIG. 4. Resonances of the decoupled electron-vibron system ($V=0$) in action space for $\gamma=1$. J_1,J_2 refer to the actions of the excitonic and vibrational systems, respectively. The straight lines represent the four lowest primary resonances, whereas the curves are level curves of the unperturbed Hamiltonian.

the resonances shift to lower bond actions and for higher resonances the distance between neighboring resonances diminishes.

As a result of the coupling, island chains corresponding to resonances develop on a Poincaré map and between these island chains lie the surviving KAM curves, corresponding to integrable quasiperiodic motion, creating complete barriers for the transport in phase space. When the coupling strength V is increased, we observe that the width of the resonance zones grows wider in action and for sufficiently large V the KAM surfaces break up. For resonance zones that are not well separated, there is an overlap leading to dynamics that becomes irregular.

Chirikov's criterion for the overlap of resonances [51] gives an analytical method to estimate a critical coupling strength $V_{\rm crit}$ for the onset of extended chaos. To apply the criterion, we first map the Hamiltonian in the vicinity of a given resonance onto an integrable Hamiltonian through a secular transformation that eliminates the resonance. The resulting Hamiltonian, when expanded to second order in the distance from the center of the resonance, becomes the pendulum Hamiltonian. From the latter one can immediately infer the width of the resonance. According to Chirikov's criterion, resonance overlap occurs when the sum of the half-width of two neighboring resonances exceeds the value for the distance between them [51]. For the Hamiltonian of Eq. (39), a resonance can be eliminated through the canonical transformation

$$F=(\theta_1+m\theta_2)I_2-\theta_1 I_1 , \tag{47}$$

giving the following relation between the old and new action-angle variables:

$$I_1=\frac{1}{m}J_2-J_1, \quad \phi_1=-\theta_1 , \tag{48}$$

$$I_2=\frac{1}{m}J_2, \quad \phi_2=\theta_1+m\theta_2 . \tag{49}$$

The transformed Hamiltonian (excluding the constant term) is

$$\bar{H}^0=mI_2[1-\tfrac{1}{2}(mI_2)]-\tfrac{1}{2}\gamma(I_1-I_2)^2 , \tag{50}$$

$$\bar{H}^1=-\epsilon 2V\sqrt{1-(I_1-I_2)^2} \times\sum_n W_n(nI_2)\cos\left\{\frac{n}{m}\left[\left[\frac{m}{n}-1\right]\phi_1+\phi_2\right]\right\} . \tag{51}$$

Close to a resonance, we retain only the slowly varying part of the perturbation connected with the angle ϕ_2. Introducing the new coordinate $\Delta I=I_2-I_2^0$ for the excursion of the action from the stationary point I_2^0, we expand Eq. (50) in a Taylor series up to second order about the stationary point. We obtain for the motion near a resonance the pendulumlike Hamiltonian

$$H=-\tfrac{1}{2}(m^2+\gamma)\Delta I^2-G_m\cos\phi_2 , \tag{52}$$

with the amplitude

$$G_m=\epsilon 2V\sqrt{1-(I_1^0-I_2^0)^2}W_m(mI_2^0) . \tag{53}$$

The center of a given resonance is determined by

$$I_2^0=\frac{m+\gamma I_1^0}{m^2+\gamma} , \tag{54}$$

where $I_1^0=I_1^0(J_1(0))$ is a constant of motion obtained from the corresponding level curve of the unperturbed Hamiltonian. The width of the mth resonance in the action variable is

$$\Delta I_m=2\left[\frac{G_m}{m^2+\gamma}\right]^{1/2} . \tag{55}$$

Using Eqs. (46), (48), (49), and (54), we evaluate the separation δ_m between the mth and $(m+1)$th resonance:

$$\delta_m=I_2^0(m+1)-I_2^0(m) =\frac{(m+1)+\gamma I_1^0(m+1)}{(m+1)^2+\gamma}-\frac{m+\gamma I_1^0(m)}{m^2+\gamma} . \tag{56}$$

The islands of neighboring primary resonances overlap when the ratio of the island's width to the separation is greater than 1, i.e., for

$$\frac{\frac{1}{2}[\Delta I_{m+1}+\Delta I_m]}{\delta_m}>1 . \tag{57}$$

From this inequality we obtain an estimate for a critical coupling constant $V_{\rm crit}$ above which extended chaotic motion is anticipated. The dependence of the critical coupling $V_{\rm crit}$ on the (initial) excitonic action J_1 is illustrated in Fig. 5. We note that for a destruction of the KAM trajectory between the two lowest resonances with $m=1$ and 2, the critical coupling $V_{\rm crit}$ increases substantially with increasing action J_1. Consequently, the more localized the excitonic energy, the less possible it is for a bond to break. On the other hand, for overlap of the higher resonances the Chirikov criterion gives critical V values which are always small, i.e., dissociation of higher excited dimer bonds should be possible for fairly small transfer integrals nearly irrespective of the location of the

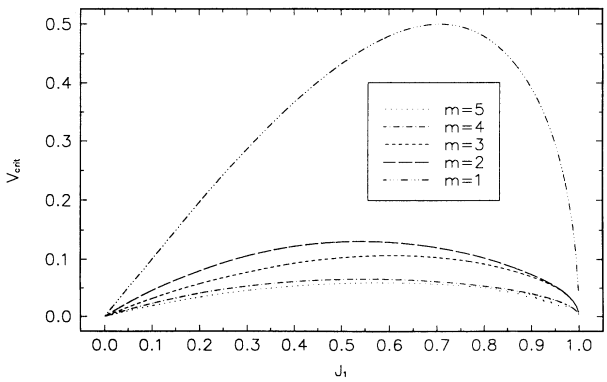

FIG. 5. The critical coupling constant $V_{\rm crit}$ determined from the resonance overlap criterion of Eq. (57) for $m=1-5$ and $\gamma=1$ as a function of the excitonic action J_1.

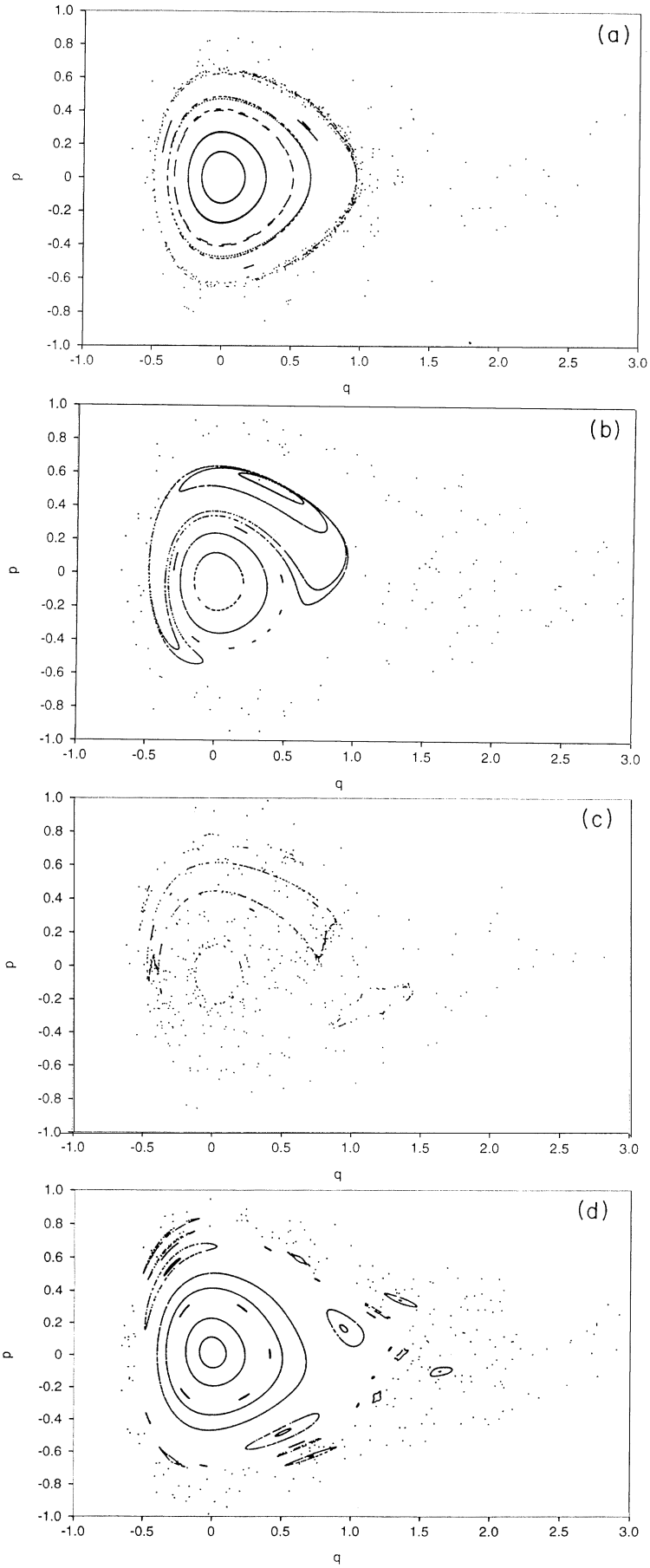

FIG. 6. Surface of section describing the coupled exciton bond-vibration dynamics in variables (p,q) for the Morse oscillator. We use the same initial conditions for the Morse oscillator in (a)–(d) and set the coupling $V=0.0216$. (a) $J_1=0.29$ and $\gamma=1$. Primarily regular behavior and only the region around the unperturbed separatrix and the $m=4$ resonance zone are filled with chaotic dynamics. (b) $J_1=0.80$ and $\gamma=1$. A large region of the $m=1$ resonance appears corresponding to periodic energy exchange between the excitonic and the vibrational degree of freedom. (c) $J_1=0.29$ and $\gamma=3$. Extended chaos except for two remaining islands of stability. (d) $J_1=0.80$ and $\gamma=3$. Some resonances are denoted by island chains.

excitonic excitation energy on the dimer.

To examine further the effects of the initial preparation of the excitonic system and of the nonlinearity, we plot in Fig. 6 the Poincaré surfaces of section calculated for two different values of the nonlinearity and for a transfer integral with $V=0.0216$. Each plot was formed from the same bond oscillator initial conditions and the initial excitonic occupation difference is $J_1(0)=0.29$ in Figs. 6(a) and 6(c) and $J_1=0.8$ in Figs. 6(b) and 6(d), representing different situations of localization of the excitonic energy. For a relatively small nonlinearity $\gamma=1$, most of the phase space is characterized by dominantly regular behavior corresponding to bounded solutions and a chaotic region mainly near the location of the unperturbed separatrix. Dissociation is indicated by the scattered points extending out towards large q values. In accordance with the predictions of the overlap criterion, the region of resonances with $m>3$ in Fig. 6(a) is already filled with chaotic solutions. For higher nonlinearity ($\gamma=3$) the character of the dynamics depends strongly on the localization of the excitation energy. In the case of a more localized exciton, the Poincaré map is still characterized by a large region of regular solutions and only a small number of initial conditions with high enough bond energy escape from the bounded region. For a more delocalized exciton, on the other hand, we observe extended chaos. Except for two islands and a small region around the origin, the phase space, even for this small coupling constant V, is already covered with irregular solutions allowing dissociation for most bond configurations.

V. CONCLUSIONS

Dissociation of molecules can be now understood as a phase space phenomenon resulting from a breakdown of classical integrability [38,6]. The dynamical systems approach, also used in the present work, utilizes Hamiltonian concepts without resorting to stochastic forces. It has the advantage of giving precise information on the exact mechanism that leads to dissociation, viz., the turnstile dynamics. It can also be utilized for obtaining quantitative information on the dissociation rates.

The basic aim of the present work has been to combine two well-known limits for a fuller understanding of the dissociation dynamics. The first limit involves the exciton transfer between two units of a molecule, whereas the second is related to the relative vibrations of the two units. The exciton transfer problem has been treated within the discrete nonlinear Schrödinger equation framework, incorporating in an approximate fashion the interaction of excitations with the local vibrations. The advantage of the DNLS approximation is that it is completely integrable for the dimer case that is relevant here [30]. For the relative molecular vibrations we chose the Morse potential since it contains all the basic physics of the bond and has been studied extensively in the past. The vibrational and excitonic problems are coupled through the intersite matrix elements since the value of the latter changes with the bond length.

The basic conclusions of our study are the following.

(i) The complete coupled system is nonintegrable, leading to ultimate dissociation for many parameter values.

(ii) The role of the nonlinear terms in the excitonic problem are essential: No dissociation is possible for $\gamma=0$. This means that the interaction of the exciton with its local vibrations actually *assists* the flow of energy from the excitonic to the intrabond degrees of freedom.

(iii) The dissociation process depends strongly on the initial preparation of the excitonic system. The bond breaks more easily when the excitation is delocalized.

(iv) Finally, in the case of extended chaos the Chirikov overlap criterion can be used to predict the onset of unrestricted dissociation.

The findings of this work can be applied to a large number of molecular dimer systems where the coupling of the excitonic degrees of freedom to local vibrations is large. In these systems local modes can occur as a result of this strong coupling. Of the several organic systems that can be studied, the linear dimer of formamide is a possible candidate for the application of our results. Extensive work has been done on this system due to its relevance to issues related to efficient propagation of energy in biological macromolecules [27]. It is possible to use the data collected for the formamide dimer and also the results obtained in this work in order to predict the dissociation rate of formamide. This prediction can be used for an independent estimation of the nonlinear coupling coefficients in the formamide dimer [52]. In addition to the relevance to molecular dimer systems, our model can also be applied to photodissociation, especially in situations when a chromophoric group is electronically energized and the energy is passed to the vibrational modes of a (weak) bond via a radiationless transition. Further work, however, needs to be done in this direction in order to establish the connection of the present approach with the standard theories of photodissociation [1–4].

ACKNOWLEDGMENTS

We wish to acknowledge partial support of Grant No. RGFY93-280 of the Texas National Research Laboratory Commission and also Grant No. ERBCHRXCT930331 of a Human Capital and Mobility Network of the European Community.

[1] K. F. Freed and Y. B. Band, in *Excited States,* edited by E. C. Lin (Academic, New York, 1977), Vol. 3.

[2] Y. B. Band, K. F. Freed, and D. J. Kouri, Chem. Phys. Lett. **79**, 233 (1981).

[3] Y. B. Band and K. F. Freed, Chem. Phys. Lett. **79**, 238 (1981).

[4] S. J. Singer, K. F. Freed, and Y. B. Band, Adv. Chem. Phys. **61**, 1 (1985).

[5] S. K. Gray, S. Rice, and D. W. Noid, J. Chem. Phys. **84**, 3745 (1986).
[6] M. J. Davis and S. K. Gray, J. Chem. Phys. **84**, 5389 (1986).
[7] W. Forst, *Theory of Unimolecular Reactions* (Academic, New York, 1973).
[8] R. B. Walker and R. K. Preston, J. Chem. Phys. **67**, 2017 (1977).
[9] S. K. Gray, Chem. Phys. **75**, 67 (1983).
[10] D. A. Jones and I. C. Percival, J. Phys. B **16**, 2981 (1983).
[11] R. B. Shirts and T. F. Davis, J. Phys. Chem. **88**, 4665 (1984).
[12] R. M. O. Galvao, L. C. M. Miranda, and J. T. Mendonca, J. Phys. B **17**, L577 (1984).
[13] R. C. Brown and R. E. Wyatt, Phys. Rev. Lett. **57**, 1 (1986).
[14] M. E. Goggin and P. W. Milonni, Phys. Rev. A **37**, 796 (1988).
[15] D. W. Noid and J. R. Stine, Chem. Phys. Lett. **65**, 153 (1979).
[16] M. E. Goggin and P. W. Milonni, Phys. Rev. **38**, 5174 (1988).
[17] D. Beige and S. Wiggins, Phys. Rev. A **45**, 4803 (1992).
[18] Y. Gu and J. M. Yuan, Phys. Rev. A **36**, 3788 (1987).
[19] D. Poppe and J. Korsch, Physica D **24**, 367 (1987).
[20] J. Heagy and J. M. Yuan, Phys. Rev. A **41**, 571 (1990).
[21] S. H. Tersigni, P. Gaspard, and S. A. Rice, J. Chem. Phys. **92**, 1775 (1990).
[22] S. K. Gray and S. A. Rice, J. Chem. Phys. **86**, 2020 (1987).
[23] P. Gaspard and S. A. Rice, J. Phys. Chem. **93**, 6947 (1989).
[24] A. A. Zembekov, Phys. Rev. A **42**, 7163 (1990).
[25] R. E. Gillilan and G. S. Ezra, J. Chem. Phys. **94**, 2648 (1991).
[26] R. E. Gillilan, J. Chem. Phys. **93**, 5300 (1990).
[27] B. M. Pierce, in *Davydov's Soliton Revisited,* Vol. 243 of *NATO Advanced Study Institute, Series B: Physics,* edited by P. L. Christiansen and A. C. Scott (Plenum, New York, 1991).
[28] T. Holstein, Ann. Phys. (N.Y.) **8**, 325 (1959).
[29] A. S. Davydov, J. Theor. Biol. **38**, 559 (1973); Sov. Phys. Rev. B **25**, 898 (1982); A. S. Davydov and N. I. Kislukha, Phys. Status Solidi B **59**, 465 (1973); Zh. Eksp. Teor. Fiz. **71**, 1090 (1976) [Sov. Phys.—JETP **44**, 571 (1976)].
[30] J. C. Eilbeck, P. S. Lomdahl, and A. C. Scott, Physica D **16**, 318 (1985).
[31] K. Lindenberg, D. W. Brown, and X. Wang, in *Far from Equilibrium Phase Transitions,* edited by Luis Garrido, Lecture Notes in Physics Vol. 319 (Springer-Verlag, New York, 1988).
[32] V. M. Kenkre and D. K. Campbell, Phys. Rev. B **34**, 4959 (1986).
[33] V. M. Kenkre, G. P. Tsironis, and D. K. Campbell, in *Nonlinearity in Condensed Matter,* edited by A. R. Bishop *et al.* (Springer, New York, 1987); G. P. Tsironis and V. M. Kenkre, Phys. Lett. A **127**, 209 (1989).
[34] D. Hennig and B. Esser, Phys. Rev. A **46**, 4569 (1992).
[35] S. Wiggins, *Global Bifurcations and Chaos: Analytical Methods* (Springer-Verlag, New York, 1988).
[36] J. Guckenheimer and P. Holmes, *Nonlinear Oscillations, Dynamical Systems, and Bifurcations of Vector Fields* (Springer-Verlag, New York, 1983).
[37] A. J. Lichtenberg and M. A. Lieberman, *Regular and Stochastic Motion* (Springer-Verlag, Berlin, 1982).
[38] S. Wiggins, *Chaotic Transport in Dynamical Systems* (Springer-Verlag, New York, 1991); S. Wiggins, Physica D **44**, 471 (1990).
[39] R. S. MacKay, J. D. Meiss, and I. C. Percival, Physica D **13**, 55 (1984).
[40] D. Bensimon and L. P. Kadanoff, Physica D **13**, 82 (1984).
[41] S. R. Channon and J. L. Lebowitz, Ann. N.Y. Acad. Sci. **357**, 108 (1980).
[42] R. S. MacKay and J. D. Meiss, Phys. Rev. A **37**, 4702 (1988).
[43] M. J. Davis, J. Chem. Phys. **83**, 1016 (1985).
[44] M. J. Davis, J. Chem. Phys. **86**, 3978 (1986).
[45] R. T. Skodjie and M. J. Davis, J. Chem. Phys. **88**, 2429 (1988).
[46] S. K. Gray and S. A. Rice, Faraday Discuss. Chem. Soc. **82**, 307 (1987).
[47] C. C. Marston and N. DeLeon, J. Chem. Phys. **91**, 3392 (1989).
[48] V. Rom-Kedar, A. Leonard, and S. Wiggins, J. Fluid Mech. **214**, 347 (1990).
[49] G. Kovacic, Physica D **51**, 226 (1991).
[50] D. Beige, A. Leonard, and S. Wiggins, Phys. Fluid A **3**, 1039 (1991).
[51] B. V. Chirikov, Phys. Rep. **52**, 263 (1979).
[52] D. Hennig and G. P. Tsironis (unpublished).